Published in final edited form as:
Dev Biol. 2008 January 1; 313(1): 408–419.

Dally Regulates Dpp Morphogen Gradient Formation by Stabilizing Dpp on the Cell Surface

Takuya Akiyama[1], **Keisuke Kamimura**[1], **Cyndy Firkus**[1], **Satomi Takeo**[2], **Osamu Shimmi**[3], and **Hiroshi Nakato**[1,*]

[1]*Department of Genetics, Cell Biology and Development, The University of Minnesota, Minneapolis, MN 55455, USA* [2]*Department of Biology, Tokyo Metropolitan University, Hachioji-shi, Tokyo 192-0397, Japan* [3]*Institute of Biotechnology, Vikki Biocenter, University of Helsinki, Helsinki, Finland*

Abstract

Decapentaplegic (Dpp), a *Drosophila* homologue of bone morphogenetic proteins, acts as a morphogen to regulate patterning along the anterior-posterior axis of the developing wing. Previous studies showed that Dally, a heparan sulfate proteoglycan, regulates both the distribution of Dpp morphogen and cellular responses to Dpp. However, the molecular mechanism by which Dally affects the Dpp morphogen gradient remains to be elucidated. Here, we characterized activity, stability, and gradient formation of a truncated form of Dpp ($Dpp^{\Delta N}$), which lacks a short domain at the N terminus essential for its interaction with Dally. $Dpp^{\Delta N}$ shows the same signaling activity and protein stability as wild-type Dpp in vitro but has a shorter half-life in vivo, suggesting that Dally stabilizes Dpp in the extracellular matrix. Furthermore, genetic interaction experiments revealed that Dally antagonizes the effect of Thickveins (Tkv; a Dpp type I receptor) on Dpp signaling. Given that Tkv can downregulate Dpp signaling by receptor-mediated endocytosis of Dpp, the ability of *dally* to antagonize *tkv* suggests that Dally inhibits this process. Based on these observations, we propose a model in which Dally regulates Dpp distribution and signaling by disrupting receptor-mediated internalization and degradation of the Dpp-receptor complex.

Keywords

Dally; heparan sulfate proteoglycan; morphogen; Decapentaplegic; *Drosophila*

Introduction

Morphogens are signaling molecules that form a concentration gradient across the developmental field and specify different cell fates by activating different sets of genes in a concentration dependent manner. Decapentaplegic (Dpp), a *Drosophila* member of bone morphogenetic proteins (BMPs), serves as a morphogen during wing development and orchestrates patterning along the anterior (A)-posterior (P) axis (Lecuit et al., 1996; Nellen et al., 1996; Entchev et al., 2000; Tanimoto et al., 2000; Teleman and Cohen, 2000; Muller et al., 2003). Dpp is expressed in a stripe of cells adjacent to the A/P compartment boundary and spreads toward the distal cells of both A and P sides. Proper formation of the Dpp gradient is

*Corresponding author, Tel: +1-612-625-1727, Fax: +1-612-626-5652, E-mail: nakat003@umn.edu.

critical for precise induction of target genes, such as *spalt* and *optomotor-blind*, that are induced at different thresholds of Dpp. However, the molecular mechanism by which the Dpp morphogen gradient is established and maintained is poorly understood.

The balance between production and degradation of morphogen molecules is postulated to critically regulate gradient formation (Wolpert, 1969). Therefore, regulation of morphogen degradation can function as a major step to determine the shape of the gradient. During *Drosophila* embryogenesis, Wingless (Wg) forms an asymmetric gradient along the A-P axis, which is achieved by asymmetric patterns of Wg protein degradation (Dubois et al., 2001). The BMP gradient also seems to be controlled by morphogen degradation. It has been suggested that extracellular Dpp is internalized by receptor-mediated endocytosis and rapidly turned over in the wing disc (Entchev et al., 2000; Teleman and Cohen, 2000). Enhancement of degradation by expressing a dominant gain-of-function form of small GTPase Rab7 resulted in a compression of the Dpp signaling range in the wing disc (Entchev et al., 2000). Furthermore, recent computational studies suggested the importance of BMP degradation during gradient formation in the wing disc (Lander et al., 2005) and in the embryo (Mizutani et al., 2005).

Several lines of evidence have shown that heparan sulfate proteoglycans (HSPGs) of the glypican family play key roles in regulation of morphogen signaling and distribution. Glypicans are glycosylphosphatidylinositol (GPI)-anchored HSPGs and consist of a protein core to which heparan sulfate (HS) chains are covalently attached. The HS chains have a variety of sulfate modifications and provide binding sites for many growth factors. Dally, one of two *Drosophila* glypicans, regulates both signaling and distribution of Dpp in the developing wing (Fujise et al., 2003; Belenkaya et al., 2004). In *dally* mutant wing discs, the Dpp gradient can not be formed properly: Dpp signaling monitored by phosphorylation of Mothers against dpp (Mad) was abnormally reduced in the receiving cells (Fujise et al., 2003). In clones of cells overexpressing Dally, Dpp signaling is elevated in a cell autonomous fashion, indicating that Dally increases the sensitivity of cells to Dpp. Thus Dally serves as a co-receptor for Dpp, but the molecular basis for its control of Dpp signaling and distribution is not yet understood.

In order to understand the roles of HSPGs in morphogen gradient formation, two molecular genetic approaches are useful. First, one can use mutant cells deficient for a HSPG to observe the consequence of losing this molecule. Recent experiments using the genetic mosaic system showed that the levels of Dpp protein were significantly reduced within glypican-deficient clones (Belenkaya et al., 2004). This phenomenon can be explained by either inhibition of Dpp movement (Dpp can not enter the *dally* mutant cells) or Dpp destabilization (Dpp is rapidly degraded in the *dally* mutant cells). An alternative and complementary approach is to study the behavior of a mutant morphogen molecule that lacks the ability to interact with HSPGs but retains all other activities of the wild-type form. For example, a truncated form of *Xenopus* BMP4 was used to study the functions of HSPGs in BMP4 morphogen distribution during embryogenesis (Ohkawara et al., 2002). BMPs possess a stretch of basic amino acid residues in their N-terminal region that is essential for interacting with heparin (Ruppert et al., 1996). The mutant BMP4 molecule lacking this N-terminal segment migrated further than wild-type BMP4 in an embryo, suggesting that HSPGs restrict BMP diffusion.

In this study, we generated a mutant form of Dpp, $Dpp^{\Delta N}$. This truncated form of Dpp lacks a short domain (seven amino acid residues) at the N terminus essential for interacting with heparin and Dally. Our results showed that $Dpp^{\Delta N}$ exhibits comparable signaling activity and in vitro protein stability to the wild-type form, but has a shorter half-life in vivo: it is more quickly internalized by cells for degradation than wild-type Dpp and therefore fails to form a normal gradient in tissue. These results strongly suggest that Dally stabilizes Dpp on the cell surface and/or in the extracellular matrix.

Materials and Methods

DNA constructs

HA-dpp$^{\Delta N}$ cDNA was constructed by introducing a small deletion in *HA-dpp* cDNA (Ross et al., 2001) using the Quickchange Site-Directed Mutagenesis Kit (Stratagene). The two PCR primers used were: 5′-CGGAACAAGCGGCACGCGAACCACGACGACATGGAG-3′ (sense primer) and 5′-CTCCATGTCGTCGTGGTTCGCGTGCCGCTTGTTCCG-3′ (antisense primer). The PCR products were cloned into two plasmid vectors: pUAST (Brand and Perrimon, 1993), a general fly transformation vector for in vivo overexpression experiments, and pBRAcpA (Cherbas et al., 1994), a S2 cell expression vector for overexpressing an inserted gene under the control of the *actin 5C* promoter.

To construct *pCaspeR hs-HA-dpp*, *HA-dpp* cDNA was amplified by PCR using the following primers: 5′-GAAGAAGGAATTCCACTCGACCATAGGAAACTTTATAAGACTG-3′ (sense primer) and 5′-GAAGAAGAGATCTGATTTCCCATCGCATTCACTCGGTTGAGTG-3′ (antisense primer). The PCR product was cloned into *Eco*RI and *Bgl*II sites of pCaspeR hs.

A transgenic RNAi construct for *dally*, *pUAST-IR-dally*, was generated as genomic-cDNA fusion construct (Kalidas and Smith, 2002). Genomic and cDNA fragments were amplified by PCR using following primers: 5′-GGGCGGCCGCACGTGCAAACTGCATCTCC-3′ (genomic sense primer), 5′-GGGCATGCGCTGTTGCTCATCGCAGAAG-3′ (genomic antisense primer), 5′-GGGCATGCGGCCCACTTTACGTTGTTC-3′ (cDNA sense primer), and 5′-GGCTCGAGACGTGCAAACTGCATCTCC-3′ (cDNA antisense primer). The genomic fragment ranges from exon 5 to exon 8 of the *dally* gene (corresponding to the sequence from 1589 to 2087 of *dally* cDNA) and contains a *Not*I site at the 5′ end and a *Sph*I site at the 3′ end. The cDNA fragment bearing the sequence from 1589 to 1998, which includes no splice donor sequence when inverted, contains a *Xho*I site at the 5′ end and a *Sph*I site at the 3′ end. Each PCR product was cloned into pBluescript. The genomic fragment digested with *Not*I and *Sph*I was ligated to the inverted cDNA fragment digested with *Xho*I and *Sph*I, and subcloned into pUAST vector.

Coimmunoprecipitation

Drosophila S2 tissue culture cells were transfected with *pActin-GAL4*, *pUAST-Myc-dally*, and *pBRAcpA-HA-dpp* or *pBRAcpA-HA-dpp$^{\Delta N}$*. After incubation at 25°C for 72 hours, the cell cultures were solubilized using lysis buffer (phosphate buffered saline [PBS] containing 2% Triton X-100, pH 7.0). The soluble fractions were incubated with protein G sepharose conjugated with rat anti-HA antibody (3F10, Roche) for 16 hours at 4°C with agitation. After incubation, precipitates were washed with wash buffer (50 mM Tris-HCl, 150 mM NaCl, and 0.2% Triton X-100, pH 7.4), and proteins bound to anti-HA antibody were eluted with SDS sample buffer. The eluted proteins were subjected to western blot analysis using mouse anti-Myc (9E10) (1:2,000, Sigma) and mouse anti-HA antibodies (12CA5) (1:5,000, Roche).

Heparin-binding assay

S2 cells were transfected with *pBRAcpA-HA-dpp* or *pBRAcpA-HA-dpp$^{\Delta N}$* constructs. After incubation at 25°C for 72 hours, the medium fractions from these cultures were collected and applied to a HiTrap Heparin column (GE Healthcare). The column was washed with 10 bed volume of PBS, and proteins retained on the column were eluted with elution buffer (1 M NaCl/PBS). The eluted protein samples were analyzed by western blot analysis using mouse anti-HA antibody (12CA5) (1:5,000, Roche).

Cell-based Dpp signaling assay

Cell-based Dpp signaling assays were carried out according to the protocol described previously (Shimmi et al., 2005). S2 cells were transfected with Flag-tagged *Mad* cDNA and incubated at 25°C for 72 hours. Separately, conditioned medium was prepared from S2 cells expressing HA-Dpp or HA-Dpp$^{\Delta N}$, and protein levels of Dpp and Dpp$^{\Delta N}$ were determined by western blotting. The *Mad*-expressing S2 cells were incubated with conditioned medium containing an equivalent amount of Dpp or Dpp$^{\Delta N}$ protein. After incubation at 25°C for 4 hours, cells were lysed in SDS sample buffer. Dpp signaling was assayed by western blot analysis using rabbit anti-pMad antibody (1:5,000, a gift from T. Tabata and P. ten Dijke; (Tanimoto et al., 2000)). Levels of total Mad protein were examined as controls using mouse anti-Flag antibody (M2) (1:1,000, Sigma).

Cell-based Dpp stability assay

Cell-based protein stability assays were performed as previously described (Bhanot et al., 1996) with some modifications. HA-Dpp and HA-Dpp$^{\Delta N}$ were expressed in S2 cells and conditioned media containing these proteins were prepared. After the relative protein levels of HA-Dpp and HA-Dpp$^{\Delta N}$ were determined by western blotting, the same amount of the two proteins were incubated at 25°C with separately prepared S2 cell cultures with or without Dally overexpression. After incubation for 30 minutes, the cells were washed with M3 insect medium (Sigma) to remove unbound HA-Dpp or HA-Dpp$^{\Delta N}$. After washing, the cells were resuspended in M3 insect medium at a density of 4×10^6 cells/ml and incubated at 25°C to allow cells to internalize and degrade Dpp or Dpp$^{\Delta N}$. After incubation for the indicated times (0–6 hours), cells were recovered and dissolved in SDS sample buffer. Supernatant fractions were also analyzed to determine whether HA-tagged proteins were released from the cells during incubation. Polyadenylic acid (Sigma) was mixed with supernatants from each time point during the experiment (0–6 hours) to give a final concentration of 10 μg/ml; an equal volume of 20% trichloroacetic acid (TCA) was added, and the samples were stored at −20°C overnight. After centrifugation, precipitates were washed with acetone to remove the residual TCA and suspended in SDS sample buffer. All samples were subjected to western blot analysis using anti-HA (12CA5, 1:5,000) as a primary antibody and IRDye800 conjugated anti-mouse IgG (1:10,000, Rockland Immunochemicals) as a secondary antibody. The relative intensity of signals for HA-Dpp and HA-Dpp$^{\Delta N}$ proteins were determined using LI-COR Odyssey Blot system (LI-COR Biosciences).

As a control, we tested protein stability in a cell-free system. HA-Dpp and HA-Dpp$^{\Delta N}$ were incubated in M3 medium at 25°C, and HA-tagged proteins were detected as described above.

Acid wash treatment

Acid washing to remove membrane-bound proteins from S2 cells was carried out as previously described (Miller et al., 2000; Liu et al., 2006) with some modifications. S2 cells with or without *thickveins* (*tkv*) RNA interference (RNAi) treatment (described below) were allowed to bind HA-Dpp for 30 minutes at room temperature as above. After washing with M3 insect medium, cells were incubated with acid wash buffer (0.2 M acetic acid and 0.5 M NaCl, pH 2.5) for 5 minutes at room temperature to strip membrane-bound proteins off the cell surface. After centrifugation, the cell fraction was suspended in SDS sample buffer, and HA-Dpp was detected by western blotting using anti-HA antibody. RNAi in S2 cells was performed as described previously (Shimmi et al., 2005). S2 cells were transfected with 15 μg of *tkv* dsRNA and incubated at 25°C for 72 hours to knock-down *tkv*.

Drosophila strains

Transformants bearing *UAS-HA-dpp$^{\Delta N}$*, *hs-HA-dpp*, or *UAS-IR-dally* were generated by P element-mediated transformation. *UAS-HA-dpp* (Ross et al., 2001) and *UAS-HA-dpp$^{\Delta N}$* were used to visualize in vivo distribution of Dpp and Dpp$^{\Delta N}$, respectively. Two *UAS-HA-dpp$^{\Delta N}$* transgenic strains (#1 and #2) that show different expression levels of HA-Dpp$^{\Delta N}$ were used. Western blotting showed that the level of HA-Dpp$^{\Delta N}$ protein expressed in *dpp>HA-dpp$^{\Delta N}$* (#2) was 5-fold higher than that in *dpp>HA-dpp$^{\Delta N}$* (#1) (Fig. S1). *UAS-HA-dpp* (A12) and *UAS-HA-dpp$^{\Delta N}$* (#1) produce indistinguishable levels of HA-tagged proteins when induced by *dpp-GAL4* driver. *dpp-GAL4*, *hh-GAL4*, and *engrailed (en)-GAL4* were used to induce expression of UAS transgenes and are described in Fly Base. Other transgenic lines used were: *UAS-dally* (Tsuda et al., 1999), *UAS-Myc-dally* (Takeo et al., 2005), and *UAS-tkv* (Tanimoto et al., 2000). All flies were maintained at 25°C except where noted.

Immunohistochemistry

Conventional immunostaining of HA-tagged proteins in third larval instar wing discs was performed as previously described (Fujise et al., 2001) using rat anti-HA antibody (3F10) (1:200, Roche). The same antibody (3F10) (1:20) was used for extracellular staining (Strigini and Cohen, 2000; Takeo et al., 2005). The Dpp activity gradient was visualized using rabbit anti-pMad antibody (1:1,000; (Tanimoto et al., 2000; Fujise et al., 2003). The primary antibodies were detected by Alexa Flour conjugated anti-rabbit IgG or anti-rat IgG antibodies (1:500, Molecular Probes).

In vivo Dpp stability assays

We used two different assays to monitor Dpp stability in vivo. For the first assay, *UAS-HA-dpp* and *UAS-HA-dpp$^{\Delta N}$* were expressed at the anteroposterior compartment boundary of the wing disc by *dpp-GAL4*. Two *UAS-HA-dpp$^{\Delta N}$* transgenic strains (#1 and #2) that express different levels of HA-Dpp$^{\Delta N}$ were used. Wing discs were dissected from late third instar larvae, and HA-Dpp and HA-Dpp$^{\Delta N}$ proteins were pulse-labeled extracellulary with rat anti-HA antibody (1:20) for 1 hour. During labeling, wing discs were incubated with the antibody at 4°C to prevent endocytosis (Mathew et al., 2005). After washing with M3 insect medium to remove unbound antibody, the discs were further incubated in medium at 25°C to allow disc cells to internalize and degrade the pulse-labeled protein. After incubation for 3 hours, the discs were fixed and stained with Alexa Flour conjugated secondary antibodies to detect extracellular Dpp and Dpp$^{\Delta N}$. All images for anti-HA staining were taken at identical settings including gain, pinhole size, dwell time, image size, and scan time. The signal intensity in the wing pouch area was measured by NIH image using the ‘Plot Profile’ function. At least 5 wing discs were used to obtain averaged values.

For the second in vivo Dpp stability assay, we generated a transgenic fly strain bearing a HA-tagged *dpp* transgene downstream of the heat-shock promoter (*hs-HA-dpp*). We first determined the time course of degradation of Dpp expressed from this transgene. *hs-HA-dpp* transgenic animals were cultured at 25°C until third instar larval stage, transcription of *HA-dpp* was induced by a heat-shock treatment (37°C for 1.5 hours), and larvae were allowed to recover at 25°C. Tracing levels of HA-Dpp along the time course revealed that Dpp levels peaked at 2–3 hours after the heat-shock (data not shown). Afterward, HA-Dpp gradually was degraded and the signals were undetectable at 8 hours after the induction.

Based on this information, we analyzed Dpp levels at 4 and 6 hours after the heat-shock treatment in wing discs from *hs-HA-dpp/+; hh-GAL4/+*, *hs-HA-dpp/UAS-dally-Myc; hh-GAL4/+*, and *hs-HA-dpp/UAS-IR-dally; hh-GAL4/UAS-IR-dally* animals. Wing discs were dissected at these times and stained with rat anti-HA antibody (3F10, 1:200) by the

conventional staining protocol. Results of Dpp staining at 4 hours after induction are presented in Figure 7, but we obtained similar results at 6 hours.

Results

The N-terminal domain of Dpp is essential for binding to Dally

A previous study demonstrated that the N-terminal segment of basic amino acid residues in *Xenopus* BMP4 is essential for its binding to heparin, and is important for its normal distribution in an embryo (Ohkawara et al., 2002). *Drosophila* Dpp also has a stretch of basic amino acid residues in the corresponding region (Ruppert et al., 1996; Ohkawara et al., 2002). To investigate the role of HSPGs in regulating Dpp signaling, we generated a truncated form of Dpp ($Dpp^{\Delta N}$) that lacks seven amino acid residues at the N-terminus (Fig. 1A). We transfected *Drosophila* S2 cells with cDNAs encoding HA-tagged Dpp (HA-Dpp) and $Dpp^{\Delta N}$ (HA-$Dpp^{\Delta N}$) and characterized proteins secreted into the conditioned media. HA-Dpp migrates in a SDS-gel as two bands of molecular size 25 K and 23 K (Fig. 1B;(Shimmi et al., 2005)). These two mature forms of Dpp protein are produced by cleavage at different positions of the Dpp precursor by furin-type proprotein convertases (Kunnapuu and Shimmi, unpublished result).

We first examined the affinities of HA-Dpp and HA-$Dpp^{\Delta N}$ for heparin using heparin-affinity column chromatography. As previously shown (Groppe et al., 1998), wild-type Dpp was retained on the heparin column. Interestingly, we found that the two HA-Dpp fragments with different molecular sizes show different heparin-binding properties: the 25 K (upper) band strongly associated with heparin, while the 23 K (lower) band was only partially retained on the column (Fig. 1B). In contrast, $Dpp^{\Delta N}$ was found exclusively in the flow-through fraction and showed no affinity for heparin (Fig. 1B), confirming that the N-terminal basic segment of Dpp functions as a heparin-binding domain. The recently mapped cleavage site for the smaller (23 K) Dpp species is within the N-terminal basic region (Kunnapuu and Shimmi, unpublished result); therefore the low affinity of the 23 K fragment for heparin is consistent with partial loss of the heparin-binding domain.

We next examined whether $Dpp^{\Delta N}$ can interact with Dally by coimmunoprecipitation experiments. As depicted in Fig. 1C, Myc-Dally co-precipitated with Dpp, indicating that Dally forms a complex with Dpp in vitro. No co-precipitation was detected in the absence of Dpp, indicating that the binding of Dally to Dpp is specific. In contrast, we could not detect binding between Myc-Dally and HA-$Dpp^{\Delta N}$ (Fig. 1C). These results indicate that the N-terminal basic region of Dpp is essential for its interaction with Dally.

In vitro characterization of $Dpp^{\Delta N}$

We evaluated other properties of $Dpp^{\Delta N}$, including its secretion and in vitro signaling activity. First, to confirm that $Dpp^{\Delta N}$ is secreted normally from a cell, we compared levels of Dpp and $Dpp^{\Delta N}$ proteins secreted by S2 cells. Western blot analysis using cell and medium fractions showed that comparable levels of HA-Dpp and HA-$Dpp^{\Delta N}$ were detected in the medium fractions (Fig. 2A), indicating that truncation of the N-terminal basic segment does not affect secretion of Dpp.

Second, we examined signaling activity of $Dpp^{\Delta N}$ by the cell-based signaling assay (Ross et al., 2001; Shimmi and O'Connor, 2003; Shimmi et al., 2005). *Mad*-expressing S2 cells were treated with Dpp or $Dpp^{\Delta N}$ for 4 hours at 25°C. Stimulation of Dpp signaling was assessed by phosphorylation of Mad. Western blotting using anti-pMad antibody revealed that $Dpp^{\Delta N}$ induced the same level of Mad phosphorylation as Dpp (Fig. 2B). This result demonstrated that the N-terminal basic domain is not required for Dpp signaling activity.

Phenotypes induced by overexpression of *dpp* and *dpp$^{\Delta N}$*

We assessed in vivo activities of Dpp and Dpp$^{\Delta N}$ by expressing them using the GAL4/UAS system. To allow quantitative comparison of the phenotypes, we used two transgenic lines, *UAS-HA-dpp* (12A) and *UAS-HA-dpp$^{\Delta N}$* (#1), which produce comparable levels of HA-tagged molecules when induced by the same GAL4 driver (Fig. S1). Expression of *HA-dpp* using *dpp-GAL4* at 25°C caused pupal lethality in all animals due to the overdose of *dpp* (Fig. 3A). In contrast, under the same conditions, 43% of *dpp$^{\Delta N}$*-expressing animals survived until the adult stage. When animals were reared at 18°C, lethality induced by expression of *dpp* and *dpp$^{\Delta N}$* was negligible. At this temperature, 66% of the *dpp*-expressing animals exhibited a wing outgrowth phenotype (Fig. 3B). Expression of Dpp$^{\Delta N}$ induced the same phenotype with much lower penetrance: only 10% of the animals expressing *dpp$^{\Delta N}$* showed the wing outgrowth (Fig. 3B). Thus, the in vivo activity of Dpp$^{\Delta N}$ is significantly weaker than that of wild-type Dpp despite the similar in vitro activities of these molecules.

Extracellular distribution of Dpp and Dpp$^{\Delta N}$ in the wing disc

Since Dpp$^{\Delta N}$ failed to interact with Dally, which affects the shape of the Dpp gradient, we examined gradient formation by Dpp$^{\Delta N}$ in vivo. The wing discs from *dpp>HA-dpp* (12A) and *dpp>HA-dpp$^{\Delta N}$* (#1) animals were stained with anti-HA antibody using conventional and extracellular staining protocols. We observed indistinguishable levels and patterns of HA-Dpp and HA-Dpp$^{\Delta N}$ by the conventional staining protocol, suggesting that both proteins are synthesized at similar levels (Fig. 4A and B).

In contrast, we found that the patterns of extracellular Dpp and Dpp$^{\Delta N}$ staining were remarkably different. In the extracellular staining method, the primary antibody is incubated with the tissue before fixation (Strigini and Cohen, 2000). Under this condition, the antibody is only able to access extracellular antigens. Using this protocol, we observed that wild-type Dpp is widely spread and forms a long-range gradient along the entire length of the anterior-posterior axis of the wing disc (Fig. 4C; (Belenkaya et al., 2004)). We found that signals for Dpp$^{\Delta N}$ in the extracellular space were significantly weaker than those of Dpp (Fig. 4D). Intensity plots of signals for extracellular Dpp and Dpp$^{\Delta N}$ revealed a shallow gradient of Dpp$^{\Delta N}$ (Fig. 4E). Thus, Dpp$^{\Delta N}$ failed to form a normal concentration gradient and its level in the extracellular space was very low despite its normal level of synthesis. In summary, the N-terminal basic domain of Dpp that is required for binding to Dally is essential for Dpp's normal distribution in a tissue.

Stability of Dpp$^{\Delta N}$ protein in vitro

The weak extracellular staining of Dpp$^{\Delta N}$ suggested several possible molecular defects of this mutant protein. For example, Dpp$^{\Delta N}$ may not be secreted properly into the extracellular space, but we thought that defective secretion was unlikely since we observed that Dpp$^{\Delta N}$ is secreted normally in S2 tissue culture cells (Fig. 2A). Alternatively, it may fail to be retained at the cell surface and may be lost by diffusing away or by degradation. To further characterize Dpp$^{\Delta N}$, we analyzed the retention and stability of Dpp$^{\Delta N}$ on the cell surface using a cell-based protein stability assay (Bhanot et al., 1996). When HA-Dpp or HA-Dpp$^{\Delta N}$ is incubated for up to 6 hours in cell-free medium, no significant degradation is observed (Fig. 5A), indicating that both proteins are stable in the absence of cells. To assess the stability of these proteins on the cell surface, HA-Dpp or HA-Dpp$^{\Delta N}$ was incubated for 30 minutes with S2 cells, which express endogenous *dally* at low levels. After extensive washes, the cells were further incubated for 0-6 hours and the levels of HA-tagged proteins were monitored by western blot analysis (Fig. 5B). We observed that levels of both HA-Dpp and HA-Dpp$^{\Delta N}$ gradually declined. There was no significant difference in the rate and patterns of reduction of the two proteins.

We next used S2 cells overexpressing Dally in this assay. We observed a gradual decrease of $Dpp^{\Delta N}$ protein during the 6-hour incubation with *dally*-expressing cells (Fig. 5C), as in S2 cells without *dally* transfection. Significantly, under the same conditions, we observed much less reduction in HA-Dpp protein levels in this time frame (Fig. 5C), showing that Dpp stably remains in the cell fraction in the presence of high levels of Dally.

Two lines of evidence supported the idea that the reduction in Dpp levels is primarily due to degradation by S2 cells. First, in order to distinguish between an internalized fraction of Dpp and a fraction bound to the cell surface, we performed an acid wash to remove membrane-bound proteins from the cells (Miller et al., 2000; Liu et al., 2006). After incubation of the S2 cells with Dpp for 30 minutes, we treated the cells with acid wash buffer (0.2 M acetic acid and 0.5 M NaCl, pH 2.5) to strip membrane-bound proteins off the cell surface. We found that a majority of Dpp was detected in the cell fraction after the acid wash (Fig. S2). On the other hand, the amount of Dpp in the cell fraction was significantly decreased when receptor-mediated internalization was blocked by *tkv* RNAi. These results indicated that the major portion of Dpp protein we detect in the protein stability assay has been internalized within 30 minutes incubation by a Tkv-dependent mechanism. This is consistent with previous reports showing that BMPs are quickly internalized by receptor-mediated endocytosis (Jortikka et al., 1997; Miller et al., 2000). Second, to detect Dpp dissociated from the cell surface during the protein stability assay, we collected media used in these assays and precipitated total proteins with TCA. Western blot analysis of the precipitates showed no detectable Dpp proteins in the media (Fig. S3A). Western blotting to determine the detection limit of Dpp in this experiment demonstrated that less than 0.5% of the Dpp initially bound to the cell surface diffused into media during the protein stability assay (Fig. S3B). These observations are consistent with the idea that the reduction in the level of the Dpp proteins represents their degradation by S2 cells. However, we cannot rule out the possibility that a modest amount of Dpp proteins is released into the culture medium.

Stability of $Dpp^{\Delta N}$ in the extracellular space of the wing disc

To better understand why the $Dpp^{\Delta N}$ gradient in the wing disc differs from that of Dpp, we devised an assay system to directly compare the stability of wild-type Dpp and $Dpp^{\Delta N}$ in vivo. Extracellular HA-tagged proteins in *dpp>HA-dpp* and *dpp>HA-dpp*$^{\Delta N}$ discs were pulse-labeled with anti-HA antibody and chased for 3 hours at 25°C. After the incubation, the tissues were fixed and the distribution of the HA-tagged protein/antibody complex was monitored.

During incubation, the extracellular gradient of Dpp becomes broader, expanding toward both anterior and posterior edges (Fig. 6A and B). We also noticed an increase of punctate signals, which seem to represent internalized molecules (Fig. 6B). At 3 hours after the pulse-labeling, the total signal intensity of labeled molecules had decreased to 86% of the initial level (Fig. 6C). We found that $Dpp^{\Delta N}$ faded away much more quickly than Dpp. The total signal from the *dpp>HA-dpp*$^{\Delta N}$ (#1) discs was reduced to 39% in 3 hours (Fig. 6D–F). However, since the extracellular levels of HA-$Dpp^{\Delta N}$ in *dpp>HA-dpp*$^{\Delta N}$ (#1) wing discs were significantly lower than the levels of HA-Dpp at time 0 (Fig. 6D, see also Fig. 4D), it was difficult to compare temporal changes in the distributions of these proteins. We therefore used another transgenic line for *dpp*$^{\Delta N}$ expression, *UAS-HA-dpp*$^{\Delta N}$ (#2). Western blot analysis showed that this transgenic line produces 5-fold higher levels of $Dpp^{\Delta N}$ protein than *UAS-HA-dpp*$^{\Delta N}$ (#1) when induced by the same GAL4 drivers (Fig. S1). The intensity of extracellular signals in *dpp>HA-dpp*$^{\Delta N}$ (#2) discs was comparable to that of *dpp>HA-dpp* (12A) discs at 0 hour incubation (Fig. 6G). However, consistent with results from the *UAS-HA-dpp*$^{\Delta N}$ (#1) transgene, the level of pulse-labeled $Dpp^{\Delta N}$ decreased to 44% in 3 hours (Fig. 6H and I). Thus, deleting the domain required for interaction with Dally resulted in a shorter half-life for detectable Dpp protein in vivo. This result explains why the in vivo activity of $Dpp^{\Delta N}$ was significantly weaker than that

of Dpp (Fig. 3) even though both proteins showed the same signaling activity in vitro (Fig. 2B).

In order to confirm that lower stability of $Dpp^{\Delta N}$ is due to its failure to bind to Dally, we performed this in vivo pulse-chase experiment for Dpp-HA in *dally* mutant background. Consistent with the results of $Dpp^{\Delta N}$, we observed that signals of Dpp protein declined more rapidly in *dally* mutant wing discs (Fig. 6M–O) compared to wild-type (Fig. 6A–C). The signal intensity of pulse-labeled Dpp decreased in 3 hours to 67% in *dally* heterozygous discs (Fig. 6L) and to 44% in homozygous discs (Fig. 6O), showing a dosage-dependent effect of *dally* on Dpp stability. It is worth noting that the Dpp gradient does not extend normally in *dally* mutants (Fig. 6M–O), resembling a previously reported pattern of pMad (the activity gradient) in *dally* mutants (Fujise et al., 2003). The shrinkage of the Dpp gradient observed in *dally* mutant discs is also similar to the patterns of $Dpp^{\Delta N}$ (Fig. 6D–I). These similarities in temporal and spatial patterns of Dpp in *dally* mutant wing discs and $Dpp^{\Delta N}$ showed that the observed abnormalities of $Dpp^{\Delta N}$ can indeed be ascribed to its inability to interact with Dally. Altogether, these observations support the idea that Dally stabilizes Dpp in the extracellular space of the wing disc.

Effects of Dally on Dpp stability in the wing disc

To further analyze Dally's role in Dpp stability, we developed a second in vivo assay system to monitor Dpp degradation. In this method, Dpp was ubiquitously but transiently expressed in the wing disc using the heat-shock promoter. At 2–3 hours after a heat-shock treatment, the staining intensity of HA-Dpp reached a maximum level (data not shown). Dpp thus synthesized was gradually degraded and became hardly detectable around 8 hours after the induction. Fig. 7B shows a wing disc dissected from a *hs-HA-dpp* animal at 4 hours after the heat-shock treatment and labeled with anti-HA antibody using the conventional staining protocol.

To determine if changes in the *dally* dosage affect levels of Dpp protein, we reduced *dally* expression by inducing a *dally* transgenic RNAi in the posterior compartment using *hh-GAL4* and monitored HA-Dpp. We observed a striking reduction of the HA-Dpp levels in the posterior cells at 4 hours after a heat-shock pulse (Fig. 7C). We also assessed Dpp stability in a disc where *dally* was overexpressed by *hh-GAL4*. In contrast to the *dally* RNAi treatment, a high level of Dpp protein remained in the posterior compartment, suggesting that *dally* overexpression decreased the rate of reduction of Dpp protein (Fig. 7D). Thus, these two assays consistently showed that Dally slows down the rate of disappearance of Dpp and that the Dally dosage critically affects Dpp stability in vivo.

Dally antagonizes Tkv in Dpp gradient formation

Previous studies suggested that receptor-mediated endocytosis plays a major role in Dpp degradation (Entchev et al., 2000; Teleman and Cohen, 2000). Reducing the level of the type I receptor encoded by *tkv* seems to reduce the Dpp degradation rate; the Dpp activity gradient visualized by pMad-specific antibody extends to more posterior cells (Fig. 8B). If Dally stabilizes Dpp by inhibiting its endocytosis, *dally* and *tkv* may have opposite effects on the Dpp gradient. In fact, *dally* mutant wing discs show a shrunken gradient (Fig. 8C; (Fujise et al., 2003)), which is the opposite phenotype of *tkv* mutant discs. We also found that the phenotypes of *tkv* and *dally* mutants were mutually suppressed, so that the normal gradient was restored in *tkv*/+*; dally/dally* discs (Fig. 8D). Thus, the relative levels of Dally and Tkv appear to be important for maintaining the normal gradient, rather than total amount of these molecules.

We also examined the effects of elevating the levels of Dally and/or Tkv on the pMad pattern. When *dally* was overexpressed using *en-GAL4*, pMad levels were increased in the posterior

compartment (Fig. 8E). This phenotype can be explained by the increased sensitivity of cells to Dpp signaling due to the increased levels of Dally. In contrast, *tkv* overexpression limits Dpp movement, restricting pMad staining to several rows of posterior cells neighboring the anteroposterior compartment border (Fig. 8F; (Lecuit and Cohen, 1998;Tanimoto et al., 2000)). Coexpression of *dally* suppressed the pMad phenotype caused by *en>tkv*, expanding the high-pMad region to more posterior cells (Fig. 8G). Furthermore, a *tkv* mutation could also suppress a *dally* phenotype in the adult wing: *tkv* heterozygosity completely rescued the defective wing vein V of *dally* mutants (data not shown). Altogether, these results indicated that Dally co-receptor antagonizes the effect of Tkv receptor on Dpp signaling.

Discussion

The Dpp pathway is regulated by multiple cell-surface and extracellular factors (O'Connor et al., 2006). In the developing wing, Dally is one of the key molecules that modulate Dpp signaling. It affects the shape of the Dpp ligand gradient (protein distribution) as well as its activity gradient (spatial patterns of signaling activity) (Fujise et al., 2003; Belenkaya et al., 2004). Dally and Dpp expressed in S2 tissue culture cells are coimmunoprecipitated, suggesting that Dally forms a complex with Dpp (Fig. 1C; (Kirkpatrick et al., 2006)). We also observed that Dally colocalizes with Dpp and Tkv in cells (Akiyama and Takeo, unpublished result). In addition, we previously demonstrated that Dally enhances Dpp signaling in a cell autonomous fashion (Fujise et al., 2003). These findings suggest that Dally acts as a Dpp co-receptor at least in some developmental contexts (Kramer and Yost, 2003). Interestingly, however, in embryos and in imaginal disc cells close to Dpp-expressing cells, Dpp can mediate signaling without Dally, indicating that HS is not absolutely required for all BMP-dependent processes in vivo.

We demonstrated that $Dpp^{\Delta N}$, which does not bind to heparin, failed to interact with Dally. The easiest interpretation of this result is that wild-type Dpp interacts with Dally via its HS chains. However, a recent study using Surface Plasmon Resonance showed that binding of BMP4 to Dally is not fully inhibited by excess HS (Kirkpatrick et al., 2006). Also, a mutant form of Dally, which does not undergo HS modification, is able to significantly rescue *dally* mutant phenotypes. These findings suggest that the BMP-glypican interaction is not entirely dependent on the HS chains. One possible explanation for the failure of $Dpp^{\Delta N}$ to bind to Dally is that Dpp normally binds to Dally through both the HS chains and its protein core, and $Dpp^{\Delta N}$ has reduced affinities for both sites.

Although $Dpp^{\Delta N}$ lacks the ability to interact with Dally, it shows normal in vitro protein stability and signaling activity. Therefore, this truncated form of Dpp provided a powerful system to gain insight into the functions of Dally in distribution and signaling of the Dpp morphogen: we were able to use this molecule to elucidate the consequences of lacking the ability to bind HSPGs. In the wing disc, $Dpp^{\Delta N}$ cannot form a normal gradient: only a low level of $Dpp^{\Delta N}$ was detected in the Dpp-receiving cells (Fig. 4D). Notably, this pattern of $Dpp^{\Delta N}$ resembles the Dpp ligand and activity gradients observed in *dally* mutant wing discs (Fig. 6J–O, Fig. 8C; (Fujise et al., 2003)). A series of in vitro and in vivo Dpp stability assays suggested that $Dpp^{\Delta N}$ forms a shallow gradient because it is remarkably unstable in the matrix, and that the stability of Dpp depends on its interaction with Dally.

Our genetic experiments revealed that Tkv and Dally have opposite effects on Dpp gradient formation during wing development. Dally and Tkv share some common properties as components of the Dpp signaling complex: they both autonomously enhance Dpp signaling, and limit migration of Dpp by binding to Dpp protein (Lecuit and Cohen, 1998; Tanimoto et al., 2000; Fujise et al., 2003). Nevertheless, *tkv* and *dally* mutually suppress one another's pMad gradient phenotypes. Consistent with the genetic interactions observed in *dally* and *tkv* mutants,

the pMad phenotype produced by overexpression of *tkv* was significantly restored by coexpression of *dally*. These observations indicate that *dally* antagonizes *tkv* in Dpp signaling. Since it has been proposed that Tkv promotes Dpp degradation by receptor-mediated endocytosis (Entchev et al., 2000; Teleman and Cohen, 2000), *dally* may stabilize Dpp by inhibiting this process.

Altogether, our studies suggest that Dally serves as a co-receptor for Dpp and regulates its signaling as well as gradient formation by disrupting the degradation of the Dpp-receptor complex. In this model, the Dpp signaling complex with Dally co-receptor would remain longer on the cell surface or in the early endosomes to mediate signaling for a prolonged period of time. In contrast, in the absence of Dally, the complex would be relatively quickly degraded. This possible role of Dally can account for the shrinkage of the Dpp gradient in *dally* mutant wing discs (Fujise et al., 2003). However, we cannot exclude the possibility that $Dpp^{\Delta N}$ is lost from the cell surface by lack of retention and further diffuses away.

A previous kinetic analysis of FGF degradation in cultured mammalian vascular smooth muscle cells also showed that HSPG co-receptors can enhance FGF signaling by stabilizing FGF (Sperinde and Nugent, 2000). In these cells, the intracellular processing of FGF-2 occurred in stages: low molecular weight (LMW) intermediate fragments accumulated at the first step. Blocking HS synthesis by treatment of cells with sodium chlorate substantially reduced the half-life of these LMW intermediates, indicating that HSPGs inhibit a certain step of the intracellular degradation of FGF-2. HSPGs have also been implicated in the endocytosis and degradation of Wg (Marois et al., 2006). Wg protein is endocytosed from both apical and basal surfaces of the wing disc and degraded by cells to down-regulate the levels of Wg protein in the extracellular space. Marois et al. (2006) proposed that Dally-like (Dlp), the second *Drosophila* glypican, regulates the Wg gradient by stimulating the translocation of Wg protein from both the apical and basal membranes to the lateral side, a less active region of endocytosis, thereby inhibiting degradation of Wg protein.

Interestingly, $Dpp^{\Delta N}$ behaved differently in vivo from the previously reported mutant *Xenopus* BMP4 lacking the heparin-binding site (Ohkawara et al., 2002). Although the action range of BMP4 is restricted to the ventral side during *Xenopus* embryogenesis, the truncated BMP4 migrated further in the embryo. In addition, heparitinase treatment of embryos also resulted in long-range diffusion of BMP4. These findings led to the conclusion that HSPGs trap BMP4 in the extracellular matrix to restrict its distribution in the *Xenopus* embryo. This activity of HSPGs seems to be opposite to that of Dally in the Dpp receiving cells of the *Drosophila* wing, where the major role of Dally is to stabilize Dpp protein. In general, ligands that fail to be retained on the cell surface can have any of the following fates: they may (1) migrate further and act as a ligand somewhere else, (2) be degraded by extracellular proteases, or (3) be internalized by endocytosis and degraded intracellularly. Theoretically, a mixture of all these phenomena can happen at the same time in a given tissue. However, which of these predominates may depend on cellular and extracellular environmental conditions such as concentrations of proteases in the matrix and the rate of endocytosis. Therefore, in the absence of HS, whether a major fraction of ligands is degraded or migrates further can be tissue-dependent, and the effects of HSPGs on BMP gradients will vary depending on the developmental context: a mutant BMP4 molecule moves further in a frog embryo, but $Dpp^{\Delta N}$ is degraded in *Drosophila* wing.

Although the results presented here support a role for HSPGs in Dpp stability, they do not rule out the possible involvement of HSPGs in migration of Dpp protein from cell to cell. The gradient of $Dpp^{\Delta N}$ is significantly narrower than that of wild-type Dpp (Figs. 4 and 6), raising the argument that HS-binding plays a role also in normal Dpp migration in a tissue. Further studies will be required to determine whether or not HSPGs affect morphogen movement. Our

study also provides new insight into functional aspects of Dpp processing. Mature forms of Dpp generated by differential cleavages are likely to show different affinities for proteoglycans in the matrix. Therefore, they may have different half-lives and/or spatial distribution patterns in vivo. The biological significance of the occurrence of differently processed forms remains to be elucidated.

Supplementary Material

Refer to Web version on PubMed Central for supplementary material.

Acknowledgements

We are grateful to T. Tabata, P. ten Dijke, M. O'Connor, and the Bloomington Stock Center for fly stocks and reagents. We thank C. Kirkpatrick for critical reading of the manuscript and helpful comments. This work was supported by research grants from NIH and Human Frontier Science Program.

References

Belenkaya TY, Han C, Yan D, Opoka RJ, Khodoun M, Liu H, Lin X. Drosophila Dpp morphogen movement is independent of dynamin-mediated endocytosis but regulated by the glypican members of heparan sulfate proteoglycans. Cell 2004;119:231–44. [PubMed: 15479640]

Bhanot P, Brink M, Samos CH, Hsieh JC, Wang Y, Macke JP, Andrew D, Nathans J, Nusse R. A new member of the frizzled family from Drosophila functions as a Wingless receptor. Nature 1996;382:225–30. [PubMed: 8717036]

Brand AH, Perrimon N. Targeted gene expression as a means of altering cell fates and generating dominant phenotypes. Development 1993;118:401–15. [PubMed: 8223268]

Cherbas L, Moss R, Cherbas P. Transformation techniques for Drosophila cell lines. Methods Cell Biol 1994;44:161–79. [PubMed: 7707950]

Dubois L, Lecourtois M, Alexandre C, Hirst E, Vincent JP. Regulated endocytic routing modulates wingless signaling in Drosophila embryos. Cell 2001;105:613–24. [PubMed: 11389831]

Entchev EV, Schwabedissen A, Gonzalez-Gaitan M. Gradient formation of the TGF-beta homolog Dpp. Cell 2000;103:981–91. [PubMed: 11136982]

Fujise M, Izumi S, Selleck SB, Nakato H. Regulation of dally, an integral membrane proteoglycan, and its function during adult sensory organ formation of Drosophila. Dev Biol 2001;235:433–48. [PubMed: 11437449]

Fujise M, Takeo S, Kamimura K, Matsuo T, Aigaki T, Izumi S, Nakato H. Dally regulates Dpp morphogen gradient formation in the Drosophila wing. Development 2003;130:1515–22. [PubMed: 12620978]

Groppe J, Rumpel K, Economides AN, Stahl N, Sebald W, Affolter M. Biochemical and biophysical characterization of refolded Drosophila DPP, a homolog of bone morphogenetic proteins 2 and 4. J Biol Chem 1998;273:29052–65. [PubMed: 9786911]

Jortikka L, Laitinen M, Lindholm TS, Marttinen A. Internalization and intracellular processing of bone morphogenetic protein (BMP) in rat skeletal muscle myoblasts (L6). Cell Signal 1997;9:47–51. [PubMed: 9067629]

Kalidas S, Smith DP. Novel genomic cDNA hybrids produce effective RNA interference in adult Drosophila. Neuron 2002;33:177–84. [PubMed: 11804566]

Kirkpatrick CA, Knox SM, Staatz WD, Fox B, Lercher DM, Selleck SB. The function of a Drosophila glypican does not depend entirely on heparan sulfate modification. Dev Biol 2006;300:570–82. [PubMed: 17055473]

Kramer KL, Yost HJ. Heparan sulfate core proteins in cell-cell signaling. Annu Rev Genet 2003;37:461–84. [PubMed: 14616070]

Lander AD, Nie Q, Wan FY. Spatially distributed morphogen synthesis and morphogen gradient formation. Math Biosci Eng 2005;2:239–62.

Lecuit T, Brook WJ, Ng M, Calleja M, Sun H, Cohen SM. Two distinct mechanisms for long-range patterning by Decapentaplegic in the Drosophila wing. Nature 1996;381:387–93. [PubMed: 8632795]

Lecuit T, Cohen SM. Dpp receptor levels contribute to shaping the Dpp morphogen gradient in the Drosophila wing imaginal disc. Development 1998;125:4901–7. [PubMed: 9811574]

Liu ZH, Tsuchida K, Matsuzaki T, Bao YL, Kurisaki A, Sugino H. Characterization of isoforms of activin receptor-interacting protein 2 that augment activin signaling. J Endocrinol 2006;189:409–21. [PubMed: 16648306]

Marois E, Mahmoud A, Eaton S. The endocytic pathway and formation of the Wingless morphogen gradient. Development 2006;133:307–17. [PubMed: 16354714]

Mathew D, Ataman B, Chen J, Zhang Y, Cumberledge S, Budnik V. Wingless signaling at synapses is through cleavage and nuclear import of receptor DFrizzled2. Science 2005;310:1344–7. [PubMed: 16311339]

Miller AF, Harvey SA, Thies RS, Olson MS. Bone morphogenetic protein-9. An autocrine/paracrine cytokine in the liver. J Biol Chem 2000;275:17937–45. [PubMed: 10849432]

Mizutani CM, Nie Q, Wan FY, Zhang YT, Vilmos P, Sousa-Neves R, Bier E, Marsh JL, Lander AD. Formation of the BMP activity gradient in the Drosophila embryo. Dev Cell 2005;8:915–24. [PubMed: 15935780]

Muller B, Hartmann B, Pyrowolakis G, Affolter M, Basler K. Conversion of an extracellular Dpp/BMP morphogen gradient into an inverse transcriptional gradient. Cell 2003;113:221–33. [PubMed: 12705870]

Nellen D, Burke R, Struhl G, Basler K. Direct and long-range action of a DPP morphogen gradient. Cell 1996;85:357–68. [PubMed: 8616891]

O'Connor MB, Umulis D, Othmer HG, Blair SS. Shaping BMP morphogen gradients in the Drosophila embryo and pupal wing. Development 2006;133:183–93. [PubMed: 16368928]

Ohkawara B, Iemura S, ten Dijke P, Ueno N. Action range of BMP is defined by its N-terminal basic amino acid core. Curr Biol 2002;12:205–9. [PubMed: 11839272]

Ross JJ, Shimmi O, Vilmos P, Petryk A, Kim H, Gaudenz K, Hermanson S, Ekker SC, O'Connor MB, Marsh JL. Twisted gastrulation is a conserved extracellular BMP antagonist. Nature 2001;410:479–83. [PubMed: 11260716]

Ruppert R, Hoffmann E, Sebald W. Human bone morphogenetic protein 2 contains a heparin-binding site which modifies its biological activity. Eur J Biochem 1996;237:295–302. [PubMed: 8620887]

Shimmi O, O'Connor MB. Physical properties of Tld, Sog, Tsg and Dpp protein interactions are predicted to help create a sharp boundary in Bmp signals during dorsoventral patterning of the Drosophila embryo. Development 2003;130:4673–82. [PubMed: 12925593]

Shimmi O, Umulis D, Othmer H, O'Connor MB. Facilitated transport of a Dpp/Scw heterodimer by Sog/Tsg leads to robust patterning of the Drosophila blastoderm embryo. Cell 2005;120:873–86. [PubMed: 15797386]

Sperinde GV, Nugent MA. Mechanisms of fibroblast growth factor 2 intracellular processing: a kinetic analysis of the role of heparan sulfate proteoglycans. Biochemistry 2000;39:3788–96. [PubMed: 10736179]

Strigini M, Cohen SM. Wingless gradient formation in the Drosophila wing. Curr Biol 2000;10:293–300. [PubMed: 10744972]

Takeo S, Akiyama T, Firkus C, Aigaki T, Nakato H. Expression of a secreted form of Dally, a Drosophila glypican, induces overgrowth phenotype by affecting action range of Hedgehog. Dev Biol 2005;284:204–18. [PubMed: 15963974]

Tanimoto H, Itoh S, ten Dijke P, Tabata T. Hedgehog creates a gradient of DPP activity in Drosophila wing imaginal discs. Mol Cell 2000;5:59–71. [PubMed: 10678169]

Teleman AA, Cohen SM. Dpp gradient formation in the Drosophila wing imaginal disc. Cell 2000;103:971–80. [PubMed: 11136981]

Tsuda M, Kamimura K, Nakato H, Archer M, Staatz W, Fox B, Humphrey M, Olson S, Futch T, Kaluza V, Siegfried E, Stam L, Selleck SB. The cell-surface proteoglycan Dally regulates Wingless signalling in Drosophila. Nature 1999;400:276–80. [PubMed: 10421371]

Wolpert L. Positional information and the spatial pattern of cellular differentiation. J Theor Biol 1969;25:1–47. [PubMed: 4390734]

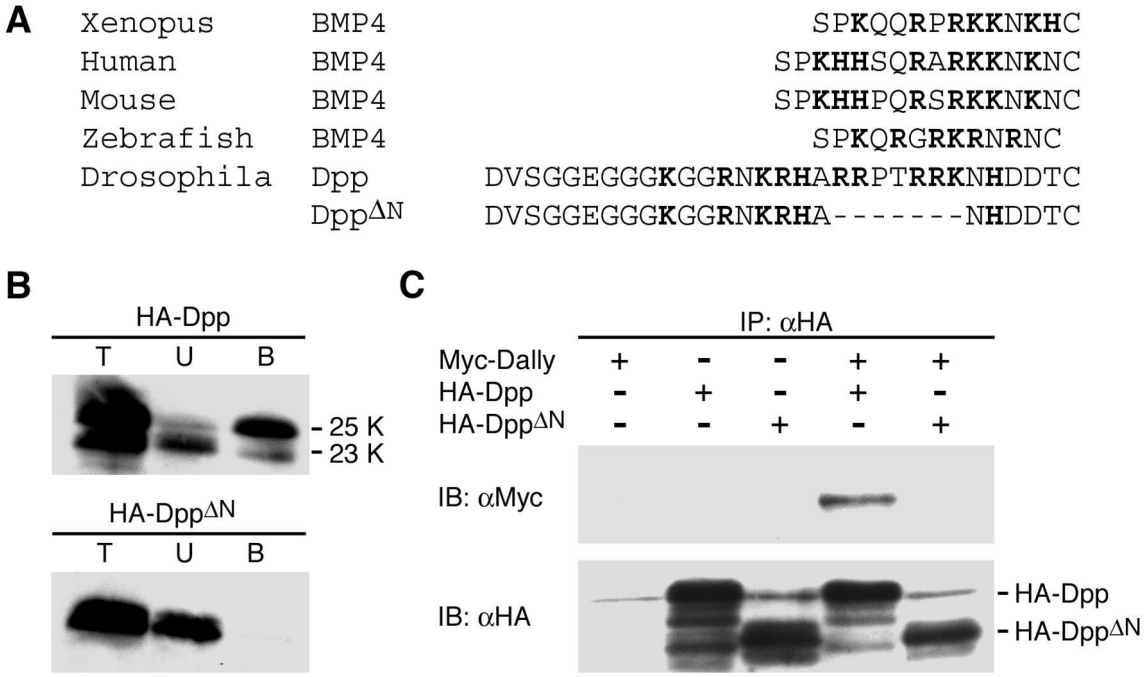

Figure 1. N-terminal basic domain of Dpp is essential for binding with Dally

(A) N-terminal amino acid sequence of vertebrate BMP4s, *Drosophila* Dpp, and a truncated form of Dpp which lacks seven amino acid residues at the N-terminus ($Dpp^{\Delta N}$). Basic amino acid residues are represented in bold. (B) Binding of Dpp and $Dpp^{\Delta N}$ to heparin. S2 cells were transfected with *HA-dpp* or *HA-dpp*$^{\Delta N}$ cDNA, and the conditioned media containing these proteins were subjected to heparin column chromatography. HA-tagged molecules in the conditioned media (T), in the unbound (U) and bound (B) fractions were detected by western blot analysis. (C) Binding of Dally to Dpp and $Dpp^{\Delta N}$. Myc-Dally and HA-Dpp proteins expressed in S2 cells were subjected to coimmunoprecipitation using anti-HA antibody as described in Materials and Methods. The precipitates were analyzed by western blot analysis using anti-Myc antibody. When Myc-Dally and HA-Dpp were coexpressed in S2 cells, Myc-Dally was recovered from the cell lysate. No binding was detected between Dally and $Dpp^{\Delta N}$. S2 cells that expressed only Myc-Dally or HA-tagged proteins were used as negative controls.

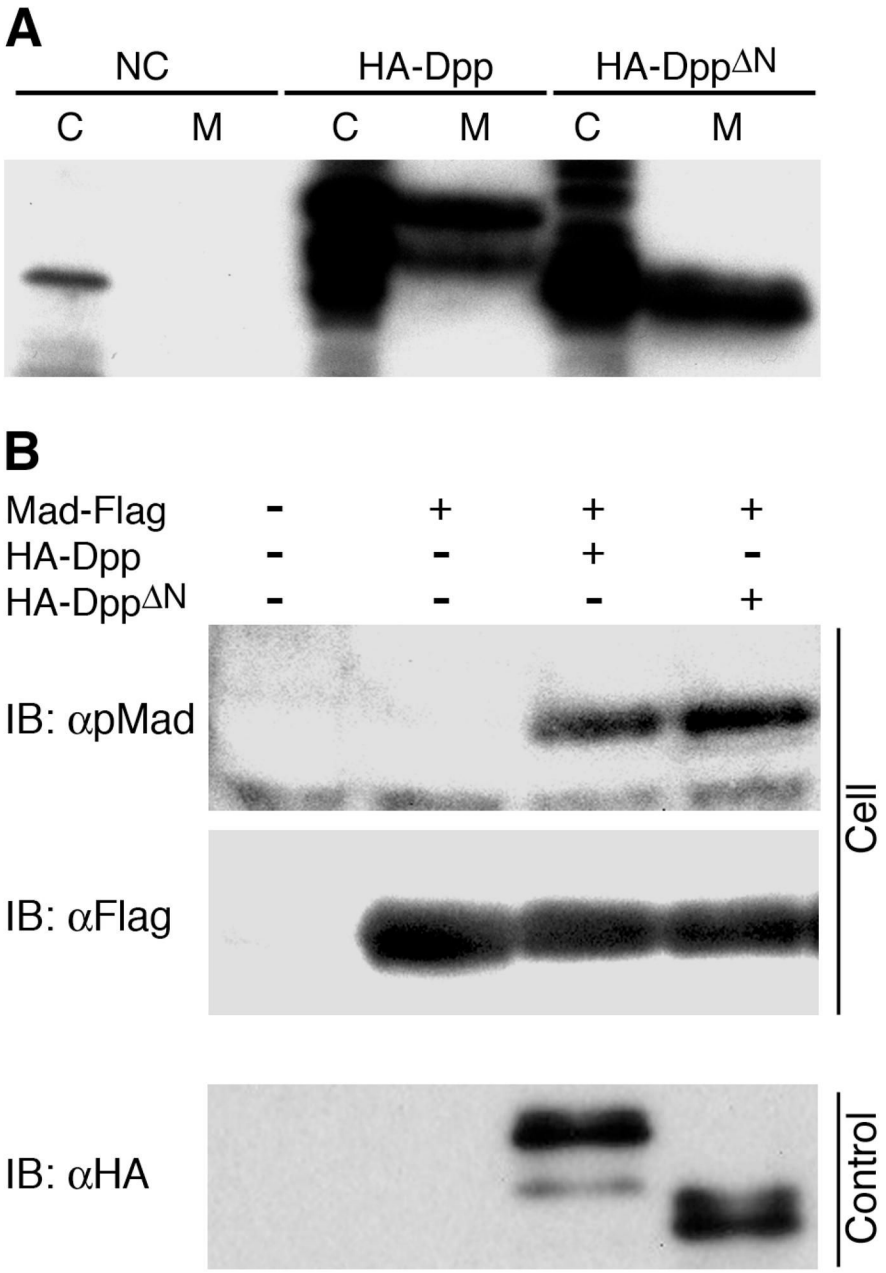

Figure 2. Secretion and in vitro signaling activity of Dpp$^{\Delta N}$

(A) Secretion of Dpp and Dpp$^{\Delta N}$. After transfection with *HA-dpp* or *HA-dpp$^{\Delta N}$* cDNA, S2 cells were incubated for 72 hours at 25°C. HA-tagged proteins in the cell (C) and medium (M) fractions were detected by western blot analysis using anti-HA antibody. Untransfected S2 cells serve as a negative control (NC). (B) In vitro signaling activity of Dpp and Dpp$^{\Delta N}$. *Mad*-expressing S2 cells were treated with Dpp or Dpp$^{\Delta N}$ for 4 hours at 25°C. Signaling activity of Dpp and Dpp$^{\Delta N}$ was assayed by western blot analysis of the cell lysate using anti-pMad antibody. Middle panel shows western blotting of the same samples using anti-Flag antibody to show total Mad protein levels. Lower panel is a control blot stained with anti-HA antibody showing the same amount of Dpp and Dpp$^{\Delta N}$ was used in this assay.

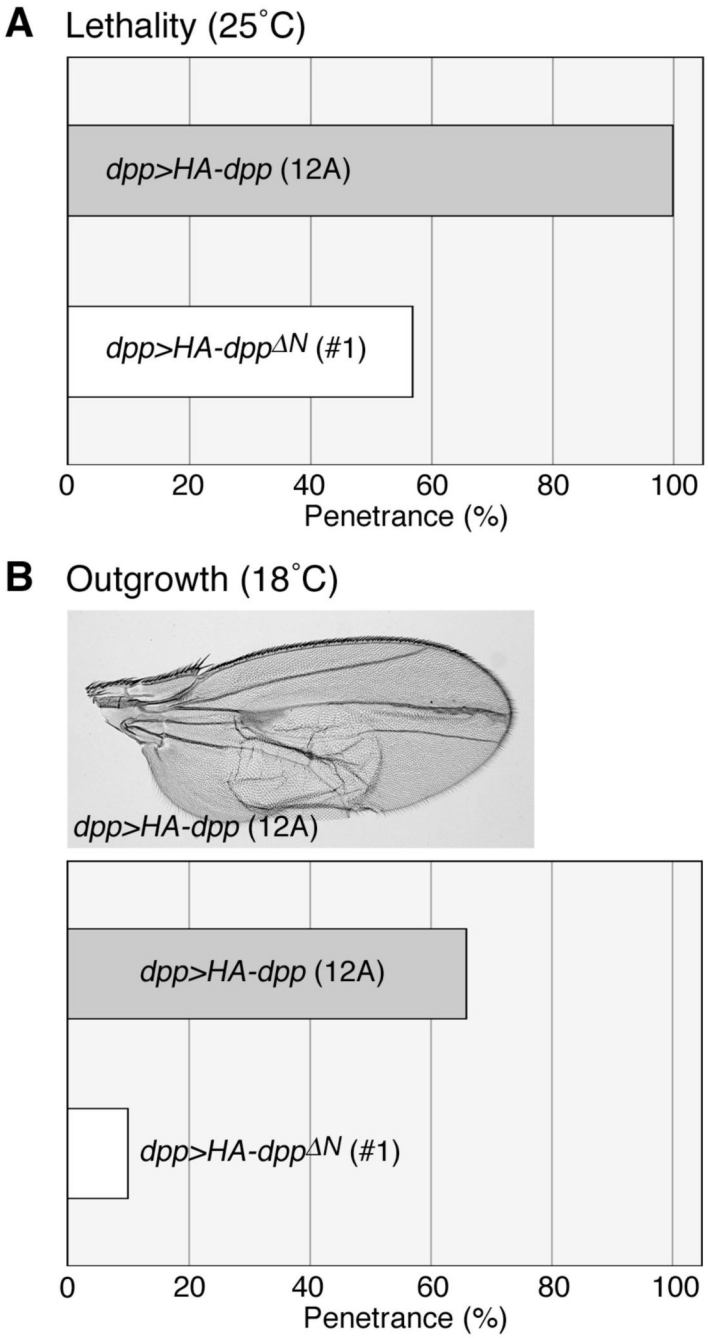

Figure 3. Comparison of in vivo activities of Dpp and Dpp$^{\Delta N}$

(A and B) Phenotypes induced by overexpression of *dpp* and *dpp*$^{\Delta N}$. Expression of *UAS-HA-dpp* (12A) or *UAS-HA-dpp*$^{\Delta N}$ (#1) was induced by *dpp-GAL4*. Bar graphs show lethality (A) and penetrance of the wing outgrowth phenotype (B) of *dpp* (grey bars)- and *dpp*$^{\Delta N}$ (white bars)-expressing animals. *dpp>HA-dpp* adult wing is shown in B.

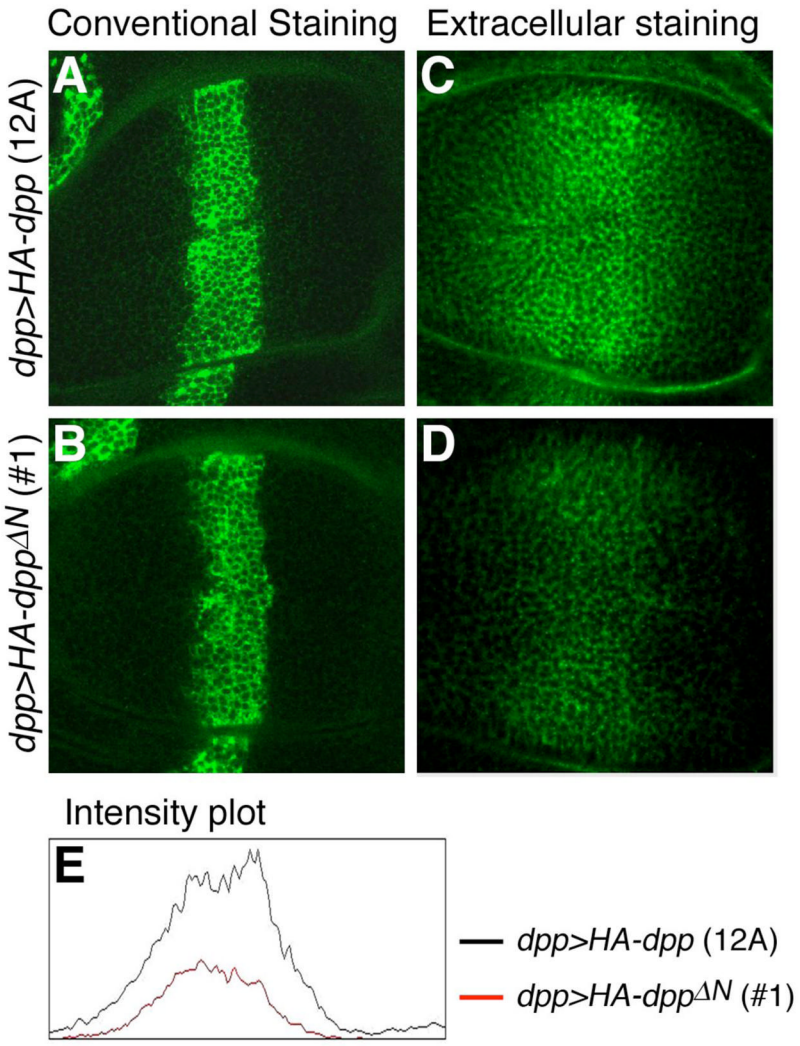

Figure 4. Distribution of Dpp and Dpp$^{\Delta N}$ in the wing discs

(A and B) Synthesis of Dpp and Dpp$^{\Delta N}$. Wing discs from *dpp>HA-dpp* (12A) and *dpp>HA-dpp$^{\Delta N}$* (#1) third instar larvae were stained with anti-HA antibody by the conventional staining protocol. Note that comparable levels of Dpp and Dpp$^{\Delta N}$ were detected in the *dpp*-expressing cells. (C–E) Extracellular distribution of Dpp and Dpp$^{\Delta N}$. HA-tagged proteins in *dpp>HA-dpp* (12A) (C) and *dpp>HA-dpp$^{\Delta N}$* (#1) (D) wing discs were labeled with anti-HA antibody by the extracellular staining protocol. Intensity profiles for extracellular signals of Dpp (black) and Dpp$^{\Delta N}$ (red) generated by NIH Image are shown in E.

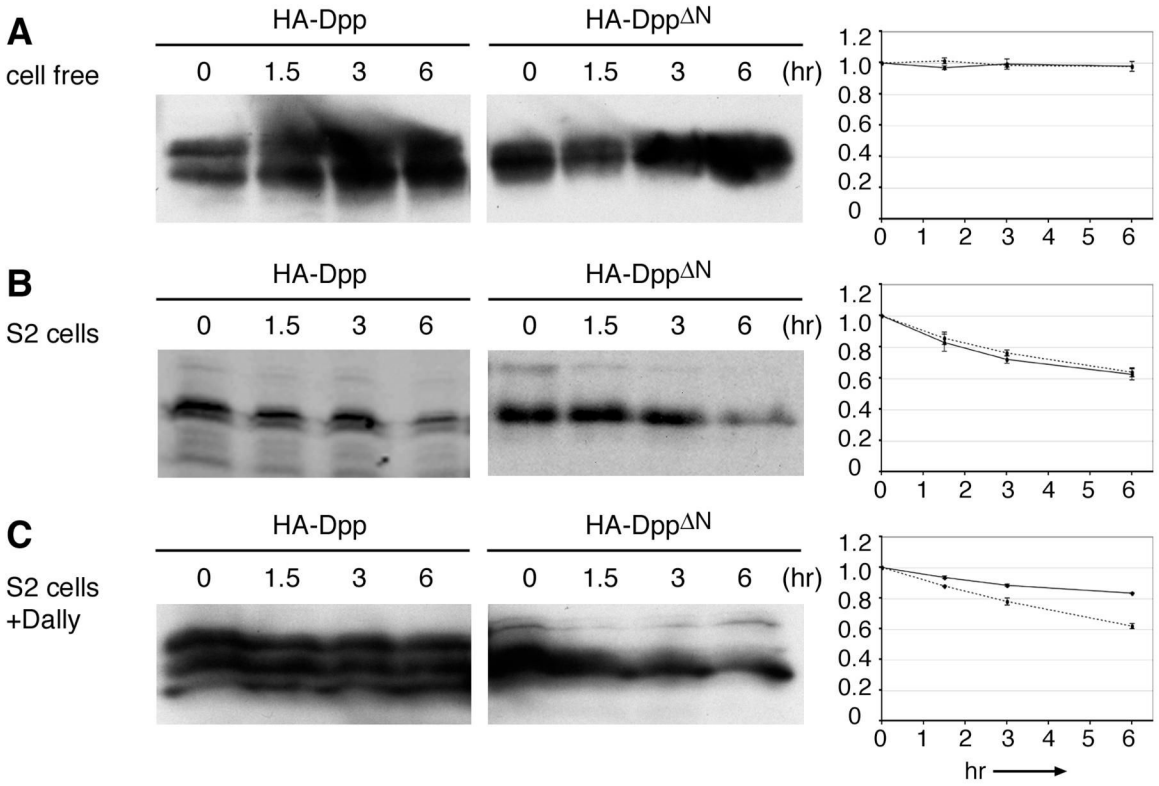

Figure 5. Stability of Dpp and Dpp$^{\Delta N}$ in S2 cells

(A) Stability of Dpp and Dpp$^{\Delta N}$ in a cell-free system. HA-Dpp and HA-Dpp$^{\Delta N}$ were incubated in M3 medium in the absence of S2 cells at 25°C. After the indicated times, HA-Dpp and HA-Dpp$^{\Delta N}$ were detected by western blot analysis using anti-HA antibody. The signal intensity at each incubation time relative to that of time 0 (shown as 1) was measured using the LI-COR Odyssey Blot system (LI-COR Biosciences) and is indicated as graphs on the right side. Relative levels of Dpp and Dpp$^{\Delta N}$ are shown by solid and dotted lines, respectively. The averaged values of results from three independent experiments are presented. (B and C) Degradation of Dpp and Dpp$^{\Delta N}$ in cell culture. HA-Dpp and HA-Dpp$^{\Delta N}$ were allowed to bind to S2 cells (B) or S2 cells overexpressing Dally (C) for 30 minutes at 25°C. After washing away unbound Dpp proteins and incubating cells for the indicated times at 25°C, the remaining proteins were detected from cell lysates as described above.

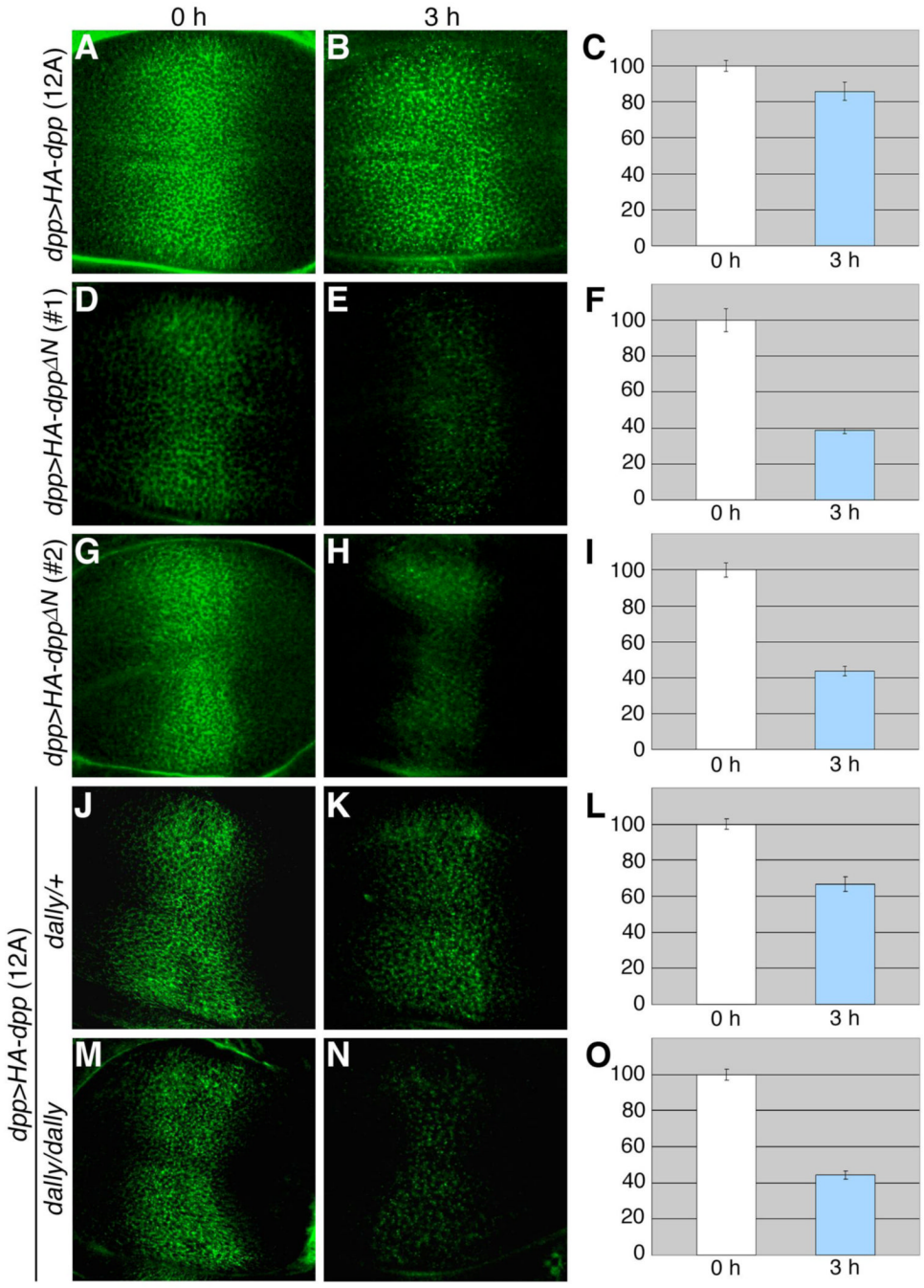

Figure 6. Stability of Dpp and Dpp$^{\Delta N}$ in the developing wing

Wing discs from UAS-HA-dpp (12A)/+; dpp-GAL4/+ (A–C), UAS-HA-dpp$^{\Delta N}$ (#1)/dpp-GAL4 (D–F), UAS-HA-dpp$^{\Delta N}$ (#2)/dpp-GAL4 (G–I), UAS-HA-dpp (12A)/+; dpp-GAL4/dally^{gem} (J–L), and *UAS-HA-dpp* (12A)/+*; dally^{gem}*, *dpp-GAL4/dally^{gem}* (M-O) were pulse-labeled with anti-HA antibody extracellularly, and incubated in M3 medium for 3 hours at 25° C. Images are shown for 0 (A, D, G, J, and M) and 3 (B, E, H, K, and N) hours after pulse-labeling. Total intensity of signals in the wing pouch area was measured by NIH Image. The relative intensity of signals at 3 hours compared to 0 hours (100%) is shown by bar graphs (C, F, I, L, and O). Each value was calculated from results of at least 5 discs.

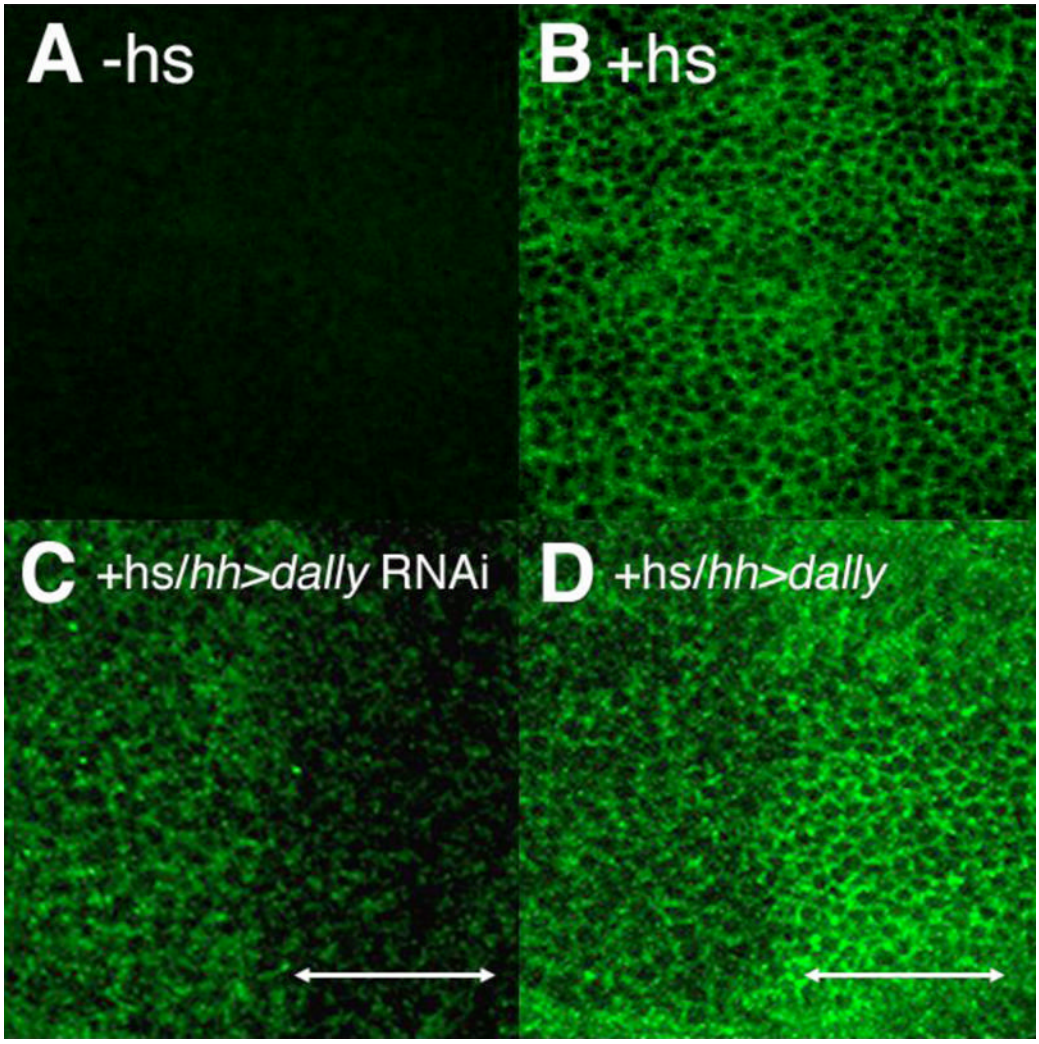

Figure 7. The effect of Dally on Dpp protein stability in the wing disc

A *hs-HA-dpp* transgenic strain was used to monitor stability of Dpp protein in the wing disc. At 4 hours after a heat-shock treatment (37°C, 90 min), wing discs were dissected from *hs-HA-dpp* larvae and Dpp protein was detected by the conventional staining protocol using anti-HA antibody. (A) A negative control staining of *hs-HA-dpp*/+; *hh-GAL4*/+ wing disc without the heat-shock induction. (B) A control disc of the same genotype where HA-Dpp expression was induced by heat-shock. (C) The same treatment was performed in a disc where a *dally* RNAi construct was expressed in the posterior cells by *hh-GAL4* driver (*hs-HA-dpp/UAS-IR-dally; hh-GAL4/UAS-IR-dally*). (D) Same as C except that *dally* was overexpressed in the posterior compartment (*hs-HA-dpp/UAS-Myc-dally; hh-GAL4*/+). White double arrow lines in C and D show regions of *dally* RNAi expression and *dally* overexpression, respectively.

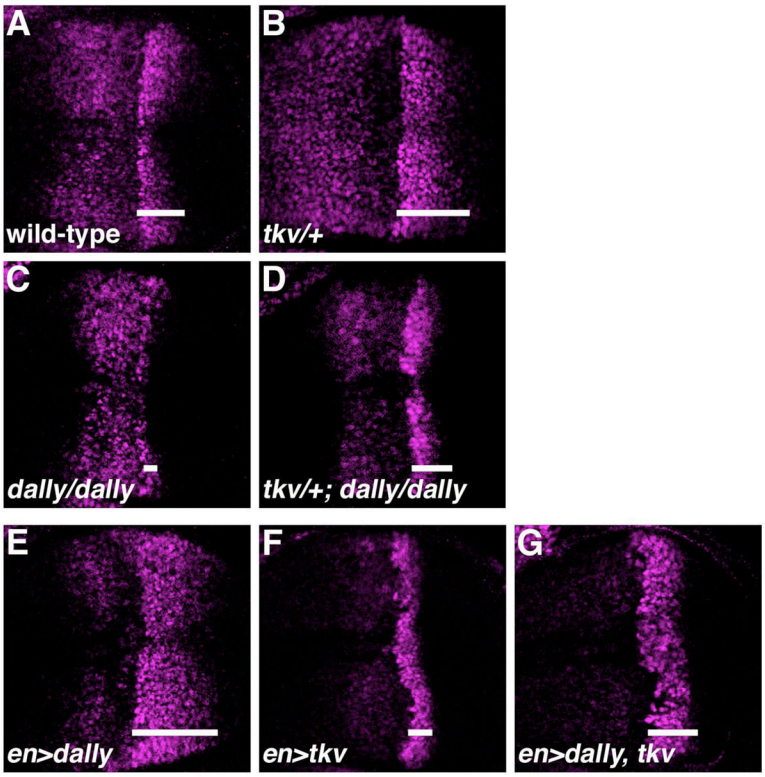

Figure 8. *dally* suppresses the effect of *tkv* on the Dpp gradient formation

Anti-pMad antibody staining of wing discs for wild-type (A), tkv^{a12} heterozygote (B), $dally^{gem}$ homozygote (C), tkv^{a12}/+; $dally^{gem}$/$dally^{gem}$ (D), *en>dally* (E), *en>tkv* (F), and *en>dally*, *tkv* (G). White bars represent domains with high levels of pMad.